

Review

Hydrogen Storage in Complex Metal Hydrides NaBH_4 : Hydrolysis Reaction and Experimental Strategies

Mirela Dragan

National Research and Development Institute for Cryogenic and Isotopic Technologies—Rm. Valcea, 4th Uzinei Str, 240050 Ramnicu Valcea, Romania; mirelad.dragan@gmail.com

Abstract: Worldwide, hydrogen is gaining ground since it is a promising alternative energy source to conventional fuels, which include fossil fuel. Thus, numerous techniques to generate hydrogen have been suggested. This literature review describes the challenges and obstacles identified through a series of the publications that target the hydrolysis of sodium borohydride. This review present several catalysts and reactor systems for the generation of hydrogen gas using the hydrolysis of sodium borohydride, selecting articles in the literature that show a promising future for this technology, although some challenges lie ahead. Sodium borohydride has been widely considered as a low-cost hydrogen storage material with high gravimetric hydrogen capacity of about 10 wt.%. However, its thermodynamic stability seriously hinders the application of sodium borohydride to obtain hydrogen. The performances of the reviewed systems of sodium borohydride hydrolysis include analysis from both the thermodynamic and kinetic points of view. The feasibility of an efficient hydrogen generation system, where a mixture of sodium borohydride and catalysts is hydrolyzed, is considered. This review aims to provide a useful resource to aid researchers starting work on the generation of hydrogen gas using the hydrolysis of sodium borohydride, so they can select the catalysts and reactor systems that best suit them. Thus far, no single catalyst and reactor system can simultaneously meet all of the required standards for efficient practical applications.

Keywords: NaBH_4 ; hydrogen; sodium borohydride; hydrogen generator; hydrogen storage; hydrolysis reaction; catalysis; kinetics; thermodynamics

Citation: Dragan, M. Hydrogen Storage in Complex Metal Hydrides NaBH_4 : Hydrolysis Reaction from Beginning to the Current Experimental Strategies. *Catalysts* **2022**, *12*, 356. <https://doi.org/10.3390/catal12040356>

Academic Editors: Loreta Tamasauskaite-Tamasiunaite and Virginija Kepeniene

Received: 27 January 2022

Accepted: 16 March 2022

Published: 22 March 2022

Publisher's Note: MDPI stays neutral with regard to jurisdictional claims in published maps and institutional affiliations.



Copyright: © 2022 by the author. Licensee MDPI, Basel, Switzerland. This article is an open access article distributed under the terms and conditions of the Creative Commons Attribution (CC BY) license (<https://creativecommons.org/licenses/by/4.0/>).

1. Introduction

The lightest element in the periodic table with $Z = 1$ is hydrogen. Hydrogen has the potential to decarbonize future energy production and eliminate dependency on fossil fuel supplies. It is known that the amount of heat released during hydrogen combustion is about 120–142 MJ/kg. This value is higher than those of petrol (about 44–46 MJ/kg), natural gas (about 42–55 MJ/kg) and wood (about 16 MJ/kg) [1]. Before hydrogen-based energy can become widely available, numerous technical challenges, especially related to its storage and transportation, still need to be addressed [2,3].

While hydrogen is an abundant chemical substance in the universe, it is not found naturally on our planet. The greatest hydrogen quantities are in water. Commonly, hydrogen gas is generated by steam reforming of hydrocarbons or by coal gasification, but these methods cause inevitable emissions of CO_2 , leading to the greenhouse effect. Given these environmental concerns, hydrogen gas generation technologies have been developed using other technologies such as water electrolysis, which exploit the renewable power from wind turbines and solar cells, but the energy efficiency of these systems is low [4,5].

Among the promising hydrogen storage material categories are metal hydrides and chemical hydrides. Both material categories depend upon catalysis to improve their kinetics. Chemical hydrides have large storage capacities for hydrogen and release, via

several chemical pathways, pure hydrogen gas. The group of chemical compounds containing the anion BH_4^- belongs to the borohydride series of hydrides. Gaseous hydrogen storage and transportation might be enabled by the utilization of borohydrides, as hydrogen-carrying molecules.

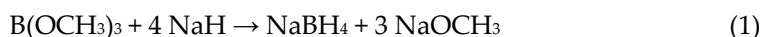
Lithium borohydride has the highest energy density as a chemical energy carrier. However, between the borohydrides, lithium borohydride, LiBH_4 , and sodium borohydride, NaBH_4 , pique the scientific community's interest the most, because they exhibit a more chemically stable composition. With respect to lithium, there is also growing concern about its availability and alternatives to lithium are sought when it involves potential industrial applications. Apart from being the sixth most abundant element within the Earth's crust, sodium, symbol Na, can be extracted from seawater, indicating that its resources are virtually limitless [6]. Some reviews of this topic have been published, but these have either focused only on catalysts [7] or on thermal decomposition, i.e., the thermal decomposition phenomenon [8].

This paper is intended to provide a short narrative review, listing in chronological order selected contributions that are available, with the goal of evaluating the possibility of set-ups for hydrogen gas generated via the hydrolysis reaction of NaBH_4 . It begins with an introduction that briefly outlines the current technological process of synthesis, technological uses including the early periods of use for hydrogen generation, along with a description of the relevant structures and thermodynamic parameters.

NaBH_4 , also known as sodium tetra-hydro-borate or sodium tetra-hydrido-borates, was discovered in the 1940s in the USA, and it has been widely studied due to its high gravimetric capacity of 10.73 wt.%. Because of the import interest at that time, the pioneering work was published much later, in 1953 [9]. However, there is more to leverage with regards to the findings of the WWII years, when NaBH_4 appeared an attractive hydrogen carrier capable of generating H_2 under ambient conditions. In addition, "the no-go recommendation" made in 2007 by the US Department of Energy regarding sodium borohydride for on-board vehicular hydrogen storage must be overcome [10]. Methods of carrying out in situ and operando hydrolysis reactions of NaBH_4 are critical to the future development of hydrogen gas generation by this method. Such developments would take hydrogen technology one step closer to the fundamental nature of the hydrolysis reaction, allowing the real-time generation of hydrogen gas by the hydrolysis reaction of NaBH_4 .

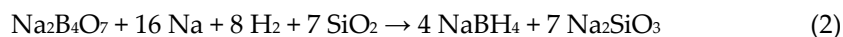
Under normal conditions, sodium borohydride is a white, solid powder. It should be mentioned that NaBH_4 is not a natural compound but a synthetic chemical. For commercial use, the processes to synthesize sodium borohydride are the Brown–Schlesinger process and the Bayer process. The Brown–Schlesinger process comprises the reaction of sodium hydride NaH, with trimethylborate $\text{B}(\text{OCH}_3)_3$, to make the product NaBH_4 and the by-product sodium methoxide NaOCH_3 . The reaction takes place with a 94% yield [11,12].

The balanced chemical equation for this reaction is given in Equation (1):



Alternately, as mentioned above, the other process employed on a commercial scale to make sodium borohydride is the Bayer process, which is a one-pot synthesis. The reaction to produce sodium borohydride by this method utilizes borax ($\text{Na}_2\text{B}_4\text{O}_7$), metallic Na, hydrogen (H_2), and silicon oxide (SiO_2), at 973 K with sodium silicate as a by-product [12,13].

The balanced chemical equation for this reaction is given in Equation (2):



This process operates via a batch mode and requires more development to produce a high yield. Currently, the Brown–Schlesinger method is still regarded as the most mature technology for the commercial production of NaBH_4 . Nevertheless, sodium

borohydride manufacture must achieve a substantial cost reduction before it can offer a low-cost material for the energy market.

After WWII, the Army Signal Corps became interested in NaBH_4 [12,13] as a potential source of field-generated H_2 for signal balloons, and various researchers investigated it as a potential propellant for rocket engines [14,15]. Traditionally, a NaBH_4 solution is used as a heat exchange medium in cooling applications. Nowadays, considering the type of end use and the area, the sodium borohydride market encompasses metal recovery; pulp, paper and textiles; pharmaceuticals; breweries; organic chemical purification; and fuel cells and hydrogen storage, as well as onboard hydrogen generation systems for portable fuel cell applications. In Figure 1. the sodium borohydride market is illustrated. With regards to its use in fuel cells with portable and transportation applications, where various operating environments are encountered, the design of the onboard hydrogen supply system must accommodate the characteristics of hydrogen generation. The hydrolysis system should be able to provide hydrogen in cold conditions, such as in winter-time, as well as at high temperatures. In practice, a low-temperature fuel cell works at temperatures around 353 K [16].



Figure 1. The market for utilization of NaBH_4 .

It should be noted that the sodium borohydride market is liable to encounter certain difficulties relating to the hazardous nature of NaBH_4 production and treatment, notably the dangers that sodium borohydride poses to human health and the natural environment [17].

Elaborating on the above-mentioned uses of sodium borohydride, NaBH_4 is used in the metal recovery of most precious metals, as well as copper and nickel, because of its effectiveness in reducing metal ions back to their free metal state [18,19]. The silver spent in photographic fixing solutions is the most metal well-known recovery process [20,21]. Sodium borohydride is also used to produce the inorganic salt, sodium dithionite ($\text{Na}_2\text{S}_2\text{O}_4$), which is used to brighten magazine and newsprint grade paper and to reduce foxing in old books and documents [22–25]. Also, within the textile industry, NaBH_4 has applications as a bleaching agent used for textiles derived from natural fibers [26]. For the pharmaceutical industry, NaBH_4 is used extensively as a reducing agent in the preparation of antibiotics such as chloramphenicol, thiamphenicol, and dihydrostreptomycin [27]. Vitamin A and some steroids are also prepared using NaBH_4 [28]. Another interesting use of NaBH_4 is in the production of light-stable hops for breweries that package their beer in green, lightly tinted or clear bottles [29].

In organic chemical purification, sodium borohydride is used to convert aldehydes and ketones to give the related alcohols; it can also improve the color, odor, and stability of many organic chemicals [30,31]. In terms of emerging markets and applications, sodium borohydride has been considered for the production of direct borohydride fuel cells, in which it is used as the primary fuel source, without any input of hydrogen or hydrocarbons [32–36]

2. Structure of NaBH₄

Sodium borohydride has a molar mass of 37.83 g/mol. It is an inorganic salt made up of a Na⁺ cation and a BH₄⁻ anion. The BH₄⁻ anion has a tetrahedral structure, with a hybridized sp³ boron atom. Studies using synchrotron diffraction on single crystals have revealed that the tetrahedral BH₄⁻ anion is bridged with the Na⁺ cation through the tetrahedral edges [37,38], as shown in Figure 2.

NaBH₄ has three stable polymorphs, denoted as α , β , and γ . Under ambient conditions, the cubic structure of NaBH₄ can be described by Fm $\bar{3}$ m or F4 $\bar{3}$ m space groups [39,40]. Based on diffraction data, the stable phase of anhydrous NaBH₄ under ambient conditions is α -NaBH₄, which is a cubic structure, isomorphous to NaCl. The structure can be described in cubic Fm $\bar{3}$ m space group symmetry [40–43]. This structure of NaBH₄ is illustrated in Figure 3.

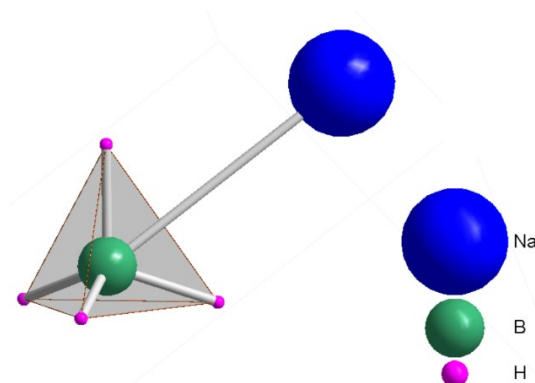


Figure 2. Tetrahedral BH₄⁻ anion bridged with the Na⁺ cation for NaBH₄.

Under conditions of increased pressure, the structure changes to the tetragonal β -NaBH₄, space group F4₂dc, at about 6.3 GPa and to the orthorhombic γ -NaBH₄, space group Pnma, at about 8.9 GPa [44,45].

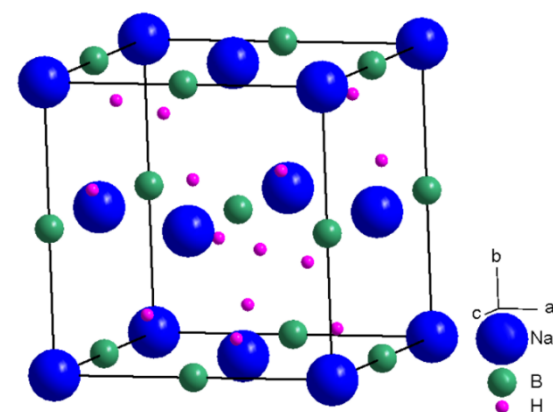
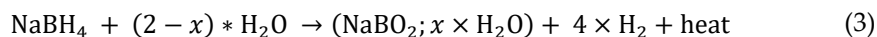


Figure 3. NaBH₄ Structure & cubic Fm $\bar{3}$ m space group symmetry.

3. Reaction Mechanism

Understanding the reaction mechanism of NaBH₄ hydrolysis is essential for reactor design. In dry air sodium borohydride is stable but it decomposes slowly in moist air. Hydrogen production is realized by the hydrolysis of borohydride in the presence of water, which is substantially aided by the presence of a catalyst, a strongly alkaline pH at 298 K, and of metaborate by-products (28 g NaBO₂/100 mL) at 298 K [46].

At room temperature, the reaction between NaBH₄ and water is very slow and results in the spontaneous release of hydrogen [47] described by the following reaction, where x is the hydration factor [48]:



where: $\Delta H_{(\text{reaction})}$ is the standard enthalpy change of formation expressed in kJ; $\sum \Delta H_{(\text{products})}$ is the sum of the standard enthalpies of formation of the products expressed in kJ/mol; $\sum \Delta H$ for reactants is the sum of the standard enthalpies of formation of the reactants expressed in kJ/mol.

Figure 4 illustrates the relationship between the main components required for the production of hydrogen through NaBH₄ hydrolysis.

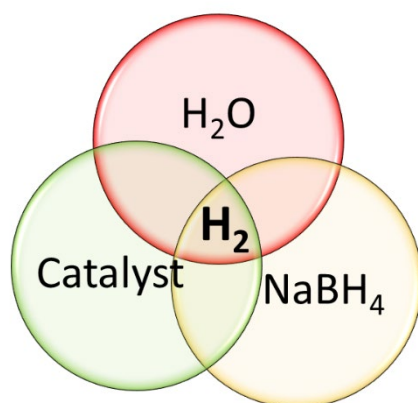


Figure 4. Hydrogen production through NaBH₄ hydrolysis.

The enthalpy of formation is the enthalpy of the hypothetical reaction required to form the species from its constituent elements in their standard states at standard pressure. ΔH is positive if a reaction adds energy to a system, i.e., is endothermic, and negative if a reaction subtracts energy from a system, i.e., is exothermic. The enthalpy of a system is a state function associated with temperature, pressure, and volume variables. Whilst undergoing temperature change, the enthalpy of the system is given by the Kirchhoff expression:

$$\Delta H = \int_{T_0}^{T_F} C_p dT \quad (4)$$

After integration

$$\Delta H = C_p \times \Delta T = C_p \times (T_F - T_0) \quad (5)$$

where: C_p is the heat capacity expressed in J/K; ΔH is the change in enthalpy expressed in J/mol; and T_0 and T_F are the standard and final temperatures expressed in K.

As can be seen in the Equation (5), the enthalpy changes proportionally to the value obtained by multiplying the temperature change and change in heat capacities of the products and reactants. The heat capacities are constant for infinitesimal variations in temperature; otherwise, the value changes with changes of temperature as seen in Figure 5.

Heat capacities are correlated using the univariate polynomial functions, as a function of temperature [49], as follows:

$$C_p(T) = \alpha_T + \beta_T \times T + \gamma_T \times T^2 + \delta_T \times T^3 + \varepsilon_T \times T^4 \quad (6)$$

where α , β , γ , δ , and ε are substance-dependent constants, obtained from dedicated tables, and T is absolute temperature, expressed in K [50].

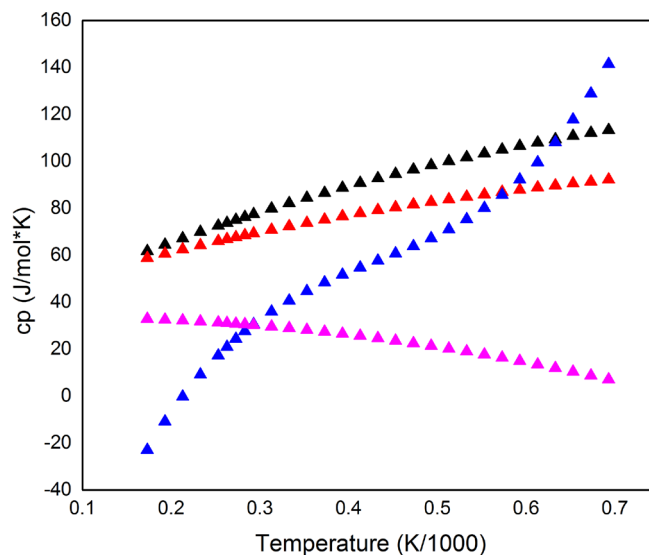


Figure 5. black = NaBH₄; red = NaBO₂; blue = H₂O; magenta = H₂.

After combining the Equations (5) and (6), the enthalpy change is described as

$$\Delta H = \int_{T_0}^{T_F} (\alpha_T + \beta_T \times T + \gamma_T \times T^2 + \delta_T \times T^3 + \varepsilon_T \times T^4) dT \quad (7)$$

And is calculated as follows:

$$\Delta H = \alpha \times (T_F - T_0) + \frac{\beta}{2} \times (T_F^2 - T_0^2) + \frac{\gamma}{3} \times (T_F^3 - T_0^3) + \frac{\delta}{4} \times (T_F^4 - T_0^4) + \frac{\varepsilon}{5} \times (T_F^5 - T_0^5) \quad (8)$$

This is the change in the enthalpy of formation caused by heating. This is added to the standard ΔH_0 enthalpy of formation at 298 K to get the enthalpy of formation, ΔH_f at T_F .

Calculations of $\Delta H_{(\text{reaction})}$ are based on the knowledge that the ΔH of NaBH₄ is -188.6 kJ/mol, ΔH of NaBO₂ is -977 kJ/mol, ΔH of H₂O is -285.8 kJ/mol, and that the enthalpy of H₂ formation is zero, because this is already the most elementary form [51]

$$\Delta H_{(\text{reaction})} = \left(-977 \frac{\text{kJ}}{\text{mol}} + 4 \times 0 \right) - \left(-188.6 \frac{\text{kJ}}{\text{mol}} + 2 \times \left(-285.8 \frac{\text{kJ}}{\text{mol}} \right) \right) = -216.8 \text{ kJ} \quad (9)$$

With the value of $\Delta H_{(\text{reaction})} = -216.8$ kJ, this system has an exothermic process, which releases heat into the environment, because the enthalpy of the products is lower in comparison to the enthalpy of the reactants. In this system, the hydrolysis reaction has a theoretical hydrogen capacity of 8.4 wt.%. However, in practice, because of the mass transfer limitation and the vaporization of water during the reaction process, it is difficult to achieve such a high hydrogen capacity. The decomposition time in which the aqueous borohydride solution hydrolyzes 50% of the sodium borohydride is expressed by its half-life $t_{1/2}$, in minutes [52]:

$$\log(t_{1/2}) = \text{pH} - (0.034 \times T - 1.92) \quad (10)$$

The decomposition rate equation shows that the reaction can be controlled by varying either or both pH and temperature. In Equation (10,) T is the temperature in K.

4. Catalysts

Several factors influence the overall amount of gaseous hydrogen produced by the reaction described within Equation (3).

Water is added to the hydride to initiate the hydrogen generating process; however, the process immediately slows down and complete conversion does not occur. In general, this reaction is known to be accelerated by low pH, catalysts, or elevated temperatures, but NaBH₄ has a thermal decomposition temperature around 673 K, so an appropriate catalyst is usually used to speed up the reaction. The catalyst modifies the energy profile to lower the activation energy required compared to non-catalyzed systems, resulting in higher reaction rates under comparable reaction conditions.

The activation energy, E_a , is an important parameter to evaluate the catalyst performance. It is calculated as the slope of the straight line on an Arrhenius plot ($\ln k$) versus the temperature factor ($1/T$). The Arrhenius equation is:

$$\ln k = \ln A - \frac{E_a}{R \times T} \quad (11)$$

where A is a pre-exponential factor, k is the H₂ evolution rate, R is the universal molar gas constant, and T is the absolute temperature.

A large number of metals have been shown to be active in the hydrolysis of NaBH₄ in alkaline solutions under various temperature conditions, including Co and Ni and their borides, as well as noble metal-based catalysts such as Pt, Pd, Pt–Ru, and Pt–Pd. To increase the reaction rate and decrease the catalyst load required, it is important to ensure a small particle size and good dispersion to maximize the contact area between the catalyst and the NaBH₄ solution.

Since noble metals are expensive and scarce, the development of noble metal-free catalysts is a subject of current research, and most of these studies are devoted to the cobalt-based catalysts [53,54], nickel based-catalysts [54,55], metal halides (NiCl₂, CoCl₂) [56], colloidal platinum [57], active carbon [58], Raney nickel [59], Ru supported on ion-exchange resin beads [60], and fluorinated particles of based materials [17], as well as cobalt and nickel borides [61]. Among them, Ru-based catalysts are known to be the most effective for promoting H₂ generation [47].

In this regard, Damjanović et al., performed a calorimetric examination of NaBH₄ hydrolysis in the presence of Co₃O₄ with different amounts of water and NaOH to study the rate of hydrolysis reaction [62]. It was found that the heat produced under various experimental conditions was steady, about 240 kJ/mol. A further finding showed that lower amounts of water resulted in a reduced reaction rate, and that the absence of NaOH resulted in poor activity and a low gravimetric capacity.

Fernandes et al., found that for the Co-B(N) catalyst, the Arrhenius plot slope of the straight line gives an activation energy of 62.4 kJ/mol on Co-B(S) [63].

Yang et al., tested the application of the CoB/SiO₂ catalyst within this reaction. The temperature of reaction was controlled. Their results showed much higher activity, 4 times greater than the unsupported CoB catalyst [64]. The hydrogen generation rate was as high as 10.586 mL H₂/(min * g_{catalyst}) at 298 K. An aqueous solution of NaOH with a pH of 13 was used for the hydrolysis reaction. The supported CoB catalyst had a greater Co⁰ content on its surface, and SiO₂ support increased the dispersion of CoB, preventing sintering. Electron donation was observed from B⁰ to Co⁰. The effect of the SiO₂ structure was to help the CoB nano-clusters achieve a high dispersion and better thermal stability, resulting in a high hydrolysis activity for the alkaline NaBH₄ solution.

Sahiner et al., tested a catalyst for the hydrolysis reaction of NaBH₄, which comprised Co nanoparticles embedded in 2-acrylamido-2-methyl-1-propansulfonic acid networks, on the order of 100 nm [65]. The activation energy for hydrogen production utilizing the

Co particles was reported to be 38.14 kJ/mol, while the activation enthalpy was 35.46 kJ/mol. The hydrolysis reaction was zero order with respect to the NaBH₄ concentration and first order with respect to the catalyst amount.

Chen et al., synthesized a recyclable cobalt nanocatalyst supported on magnetic carbon with a core-shell structure, [66] and calculated the total rate of hydrogen generation and the activation energy to be 1403 mL H₂/(min × g_{catalyst}) and 49.2 kJ/mol, respectively. These findings are comparable to the values reported for most cobalt-based catalysts for hydrogen production via hydrolysis using NaBH₄. Co/Fe₃O₄@C is a highly active catalyst for use in NaBH₄ hydrolysis hydrogen production, as indicated by its relatively low E_a value.

Ma et al., prepared Co-B hollow spheres with an inner diameter of about 260 nm and tested these as a catalyst for NaBH₄ hydrolysis [67]. The BET surface area of the Co-B hollow spheres (100.7 m²/g) is much larger than that of the Co-B nanoparticles (11.3 m²/g), providing more active sites for the catalytic reaction. The activation energies for the catalytic hydrolysis of NaBH₄ were determined to be about 45.5 and 58.6 kJ/mol for the thermal-treated Co-B hollow spheres and the amorphous Co-B nanoparticles, respectively.

Sun et al., used a new approach to produce highly dispersed metal nanoparticles of cobalt-inlaid carbon sphere catalysts, synthesized via a one-step co-pyrolysis method. They reported the calculated Arrhenius activation energy to be 32.7 kJ/mol [68].

Zhu et al., prepared carbon aerogels obtained via a boric acid-assisted hydrothermal treatment of glucose, and used these as a substrate to prepare supported cobalt nanoparticles. Their study found that the carbon aerogels/Co catalysts exhibited a relatively low activation energy of 38.4 kJ/mol [69].

Another potential catalytic metal, reported back in 2003 by Hua et al., is the nickel boride, Ni₃B, catalyst. They found that this material is active in promoting the release of H₂, with a rate of about 240 mL H₂/(min × g_{catalyst}) [70].

In addition to Raney nickel, nonmagnetic and nonpyrophoric nickel catalysts have been used in the systematic study of the borohydride-reduced metal powders. These studies revealed that, in aqueous media, a granular black material is formed from sodium borohydride and nickel (II) acetate. For double-bond hydrogenations, this material exhibited similar activity to Raney nickel. However, in ethanol, a nearly colloidal black suspension is produced, which is much more sensitive to the double-bond structure [59].

Tignol et al., examined a nickel hydrazine nitrate complex [Ni(N₂H₄)₃][NO₃]₂ with three morphologies: a hexagonal plate-like morphology, a clew-like morphology, and a disc-like morphology, in which the hexacoordinated metallic center is complexed by three N₂H₄ bidentate ligands [71]. The apparent activation energy was calculated to be about 38.7, 48.7 and 49.5 kJ/mol for the hexagonal plate-like morphology, clew-like morphology, and disc-like morphology, respectively. After hydrolysis, the complexes were supposed to be reduced because of the reducing properties of NaBH₄. The catalytic activities of the black reduced complexes were found to be about 48, 50 and 41 kJ/mol respectively.

Ghodke et al., synthesized nickel nanoparticles using the thermal plasma process [72]. At elevated temperatures, Nickel nanoparticles exhibit a first-order reaction with respect to the NaBH₄ concentration. B–O and B–OH species were found on the nickel nanoparticle surfaces after hydrolysis. Their calculations based on first-order reaction kinetics revealed an activation energy of 69.76 kJ/mol and an activation enthalpy of 67.18 kJ/mol. At 320 K, the first-order model did not fit well, which indicates that the reaction order must have shifted to an order higher than one, due to BH₄[−] ions. It appears that this synthesis method is able to produce crystalline nanoparticles with highly defined surfaces, resulting in good performance of the Ni nanoparticles.

Kaufman et al., studied the potential of NaBH₄ as a precursor fuel source for a hydrogen–oxygen (air) fuel cell with transition metals utilized as catalysts; the activation energies observed were 75 kJ/mol for Co, 71 kJ/mol for Ni, and 63 kJ/mol for Raney nickel [73].

Wei et al., used Ru/Ni foam catalysts by employing an electro-deposition method [74]. The hydrogen generation rate of the hydrolysis reaction catalyzed by the Ru/Ni foam catalyst can reach as high as 23.03 L H₂/(min × g_{catalyst}). The activation energy value of this catalytic hydrolysis process utilizing a Ru/Ni foam catalyst was estimated to be 39.48 kJ/mol, according to the authors.

Liang et al., studied the hydrolysis of NaBH₄ in the presence of a NiB/NiFe₂O₄ catalyst; they found that a hydrogen generation rate as high as 299.88 mL H₂/(min × g_{catalyst}) can be achieved for the NiB/NiFe₂O₄ catalyst when using 5 wt.% NaBH₄ solution at 298 K, which is much higher than the rate observed for pure NiB [75]. The authors observed that the use of NiFe₂O₄ can inhibit the agglomeration of NiB particles and report that the catalytic activity of NiB/NiFe₂O₄ derives entirely from the NiB active sites. However, the usage of NiFe₂O₄ support created more active sites for NiB via the dispersion of NiFe₂O₄ and the interaction between NiFe₂O₄ and NiB. They further report that the NaBH₄ hydrolysis using the NiB/NiFe₂O₄ catalyst has an activation energy of 72.52 kJ/mol.

Amendola et al., studied a ruthenium, Ru, catalyst and found the activation energy to be about 47 kJ/mol [76].

Brown et al., reported findings on the reaction of sodium borohydride with carbon-supported platinum catalysts. According to their results, the rate of hydrogenation for the supported platinum catalysts was increased by approximately 200–400% compared to the unsaturated catalysts [77].

Liu et al., produced nano-sized particles of platinum and ruthenium uniformly dispersed on the surfaces of LiCoO₂ particles using a microwave-assisted polyol process, and studied their potential as a catalyst for borohydride hydrolysis [78]. The activation energies of the various hydrogen generation reactions were calculated to be 70.4 kJ/mol for Pt/LiCoO₂ and 68.5 kJ/mol for Ru/LiCoO₂.

Chen et al., studied a Co–B catalyst, synthesized using ion exchange and chemical reduction methods, for the NaBH₄ hydrolysis reaction [79]. The ion exchange resins IR-120 and TP-207 had replaced the protons, using Co²⁺ as the ion exchange method. The amount of Co²⁺ exchanged to the resin was evaluated by measuring the concentration of Co²⁺ or H⁺. The objective of the ion exchange step was to achieve an equilibrium saturated capacity of Co²⁺ on the resin surface. In this work, an on-line method with a pH meter was used to measure the proton concentration. The IR-120 and TP-207 resins reached equilibrium after 20 and 40 min of ion exchange, respectively. The activation energy required for the NaBH₄ hydrolysis reaction using this catalyst was calculated to be 66.32 kJ/mol.

Liang et al., examined a catalyst of ruthenium supported on graphite (Ru/G) to generate hydrogen from a sodium borohydride (NaBH₄) solution [80]. The rate of hydrogen generation was about 32.3 L H₂/(min × g_{catalyst}) in a 10 wt.% NaBH₄ + 5 wt.% NaOH solution. This value is similar to that of other noble catalysts that have been studied. The calculated activation energy for hydrolysis of sodium borohydride was about 61.10 kJ/mol for the Ru/G catalyst.

Senliang et al., investigated theoretical support for seawater hydrogen production in coastal areas. The authors focused on the kinetics of NaBH₄ hydrolysis catalyzed by phosphotungstic acid, H₃PW₁₂O₄₀. Phosphotungstic acid is a kind of polyoxometalate with strong acid properties and it was selected as the active component of the catalyst [81]. Activated carbon-supported catalysts were prepared by impregnation with different percentages of phosphotungstic acid. Activated carbon offers versatility, high specific surface area, and large pore size. When using 2.5 wt.% H₃PW₁₂O₄₀/C and 4 wt.% H₃PW₁₂O₄₀/C as the catalyst, the maximum hydrogen production rate for NaBH₄ in seawater was 880 mL H₂/(min × g_{catalyst}), significantly higher than the 230 mL H₂/(min × g_{catalyst}) recorded for de-ionized water.

Microporous materials have attracted special interest as a means to encapsulate metal nanoclusters, which can function as catalysts in sodium borohydride hydrolysis [82].

Jadhav et al., synthesized and investigated as a catalyst NiCo₂O₄ hollow spheres [82]. For this, the hydrothermal method was used and a generation rate of 1000 mL H₂/(min ×

g_{catalyst}) was observed at room temperature. The activation energy for the NiCo_2O_4 hollow sphere catalyst was 52.21 kJ/mol.

Bandal et al., synthesized and investigated magnetite-multiwalled carbon nanotube nanocomposites, a magnetically recoverable catalyst for hydrolysis of sodium borohydride [83]. The production rate was 1213 mL $\text{H}_2/(\text{min} \times g_{\text{catalyst}})$ at room temperature. The activation energy of the reaction catalyzed by 5% Co-FeCNT nanocomposite was 42.79 kJ/mol.

Kim et al., prepared wüstite cobalt oxide nanorods with a high surface activity, which they named wz-CoO-NRs [84]. The hydrogen production rate was 10.367 mL $\text{H}_2/(\text{min} \times g_{\text{catalyst}})$ and the activation energy observed was 27.4 kJ/mol.

Tiri et al., used a platinum-silver nanoparticle catalyst for hydrolysis of sodium borohydride [85]. The calculated E_a was about 23.11 kJ/mol.

Zhou et al., prepared a cobalt phosphide-supported Ru particulate nanocatalyst for NaBH_4 hydrolysis [86]. The hydrogen generation rate was 9783.3 mL $\text{H}_2/(\text{min} \times g_{\text{catalyst}})$ at 298 K and the activation energy was about 45.3 kJ/mol.

Wang et al., used highly dispersed cobalt nanoparticles supported on three-dimensional graphene oxide particles as a catalyst for NaBH_4 hydrolysis [87]. The hydrogen generation rate was up to 4394 mL $\text{H}_2/(\text{min} \times g_{\text{catalyst}})$ at 298 K. The reaction activation energy was found to be about 37 kJ/mol.

Izgi et al., synthesized a Co-Cr-B/CeO₂ catalyst [88]. The hydrogen generation rate was 9182 mL $\text{H}_2/(\text{min} \times g_{\text{catalyst}})$, and the activation energy was about 35.52 kJ/mol at 303 K.

Liao et al., synthesized magnetic chitin/Cu hydrogel nanocomposites for NaBH_4 hydrolysis [89]. The E_a was calculated to be 23.21 kJ/mol.

Prasad et al., used a magnetic catalyst comprising Fe₂O₃-coated oxidized multiwalled carbon nanotubes [90]. The activation energy was about 15.92 kJ/mol.

Figure 6 summarizes the of activation energy values reported in the surveyed literature. Their corresponding reference sources are specified to the right of each symbol.

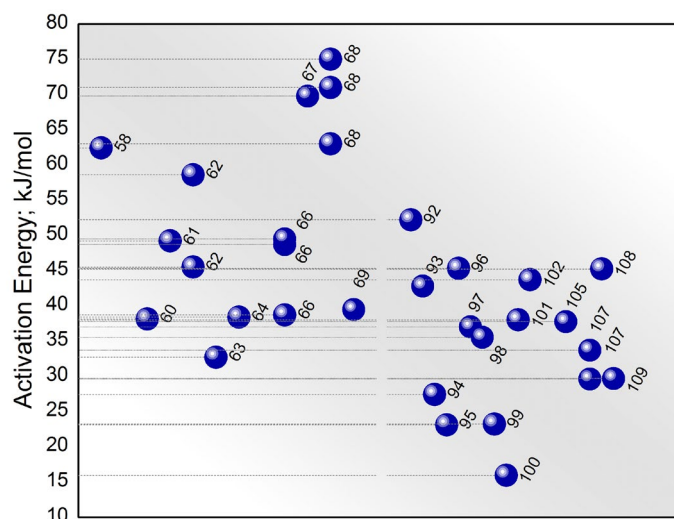


Figure 6. Summary of activation energy reported in literature, reference source specified to the right of each symbol.

Taken together, these results suggest that several catalysts, including noble metal-free catalysts, have been identified, but they have some limitations. Difficulties arise in the recovery of catalysts at the end of the reaction, which still remains an issue to be solved.

5. The Role of Method and Reactor on Carrying Out the NaBH₄ Hydrolysis Reaction

The development of sustainable systems to carry out research and tests with maximal precision, and which enable specific conclusions to be drawn regarding the production of hydrogen through NaBH₄ hydrolysis reactions, is highly multidisciplinary work. No systematic work has yet been conducted on the scale-up from experimental testing to reactor production. Reactor design is not only about safety and manageability, but also about minimizing waste, and conserving energy and water usage. In practice, a large amount of catalyst is required to increase the reaction output. For this and other reasons, the generation of hydrogen via the NaBH₄ hydrolysis reaction is cost-sensitive; increasing the catalyst amount will increase the cost of the hydrogen produced. NaBH₄ hydrolysis is exothermic, as shown in Equation (3), implying that thermal management must be improved. As such, it is not only the catalytic activity that must be considered and studied in detail.

The kinetics of the sodium borohydride hydrolysis reaction are sluggish and fall well below the theoretical capacity. This is due to the formation of by-product mixtures of hydrated metaborate with varying compositions, which require excess water. Because of this issue, such a process is inappropriate for practical gas hydrogen generators. When carrying out a reaction, multiple thermodynamic and chemical kinetic principles are involved in selecting the most appropriate conditions. Some studies recommend the Langmuir–Hinshelwood and Michaelis–Menten models, as these provide a reasonable description of behavior for a relatively wide temperature range and are therefore recommended for the modeling and design of hydrogen generation devices [91–93].

Progress has been made in this field by using many different types of operating laboratory systems, such as batch systems or continuous flow systems, as well as reactors that operate isothermally or adiabatically, to find a suitable solution.

Very early in the literature, in 1955, Brewer et al., described a simple method for producing hydrogen slowly in anaerobe jars based on the reaction of sodium borohydride with water in the presence of a catalyst [94]. These experiments showed that the reaction of sodium borohydride with water, using cobalt chloride as a catalyst, yielded about 1250 mL hydrogen in 60 min.

Building on the interest in sodium borohydride-generated hydrogen coupled with a fuel cell or a hydrogen internal combustion engine, Richardson et al., in 2005, reported a flow reactor. This reactor comprised a hollow tube with top and bottom end caps, and aimed for the continuous generation of hydrogen in the order of 500 W [18]. In their fixed bed reactor, sodium borohydride was fed through a catalyst bed. Their experiment used a series of reactors to study this approach. The hydrogen generation system consisted of a catalytic reactor, pump, feed solution vessel, by-product catch vessel, and a heat exchanger. The heat exchanger was used to cool the hydrogen gas before it entered the fuel cell. Their results demonstrated a steady-state load of 500 W and a peak capability of 2 kW.

Zhang et al., studied a 1 kWe sodium borohydride hydrogen generation system, comprising a packed-bed reactor in which sodium borohydride solution is pumped through the bed to initiate the hydrolysis reaction [95]. Using a gas–liquid separator, the gaseous hydrogen and liquid NaBO₂ solution were separated from the product stream. A large amount of water vapor entered into the high-temperature hydrogen stream, and to condense the water vapor a heat exchange process was used. In their experiment, the water vapor was further removed from the hydrogen stream through a desiccant dryer before the hydrogen stream passed through the flowmeter. Their study utilized a stainless-steel reactor equipped with a temperature probe. This design enabled the authors to accurately monitor the temperature profiles inside the reactor.

Motivated by the findings of this research using the well-instrumented 1 kWe sodium borohydride system, especially the experimental results regarding the temperature profiles inside the reactor under different controlled conditions, Zhang et al., evaluated the feasibility of such a system for vehicle applications [96]. To achieve a reliable engineering system was a challenge for the authors. They found that the hydrogen must be

conditioned before entering the flowmeter, otherwise the condensation inside the flowmeter due to mixing of high-temperature hydrogen with water vapor caused damage to the sensor. In order to remove the water vapor from the hydrogen stream, a silica gel-based desiccant dryer was used. During the reaction, the water became vaporized because sodium borohydride hydrolysis is highly exothermic. The amount of water vaporized has a strong impact on the temperature distribution inside the reactor and the chemical kinetics. Therefore, it was very important for this work to measure the relative humidity for different conditions for reactor modeling purposes. The authors used the condensate flow rate to estimate the relative humidity by assuming that the hydrogen stream coming out of the heat exchanger was saturated at the exit temperature. Because most hydrolysis reactions are exothermic, the reaction heat has to be removed from the system continuously to prevent thermal runaway. Continuous removal of reaction products is crucial in any flow system.

Oronzio et al., designed a portable fuel cell power generator with reduced weight and size [97]. The authors continued to develop and optimize a magnetic-containment reactor and a specific catalyst for hydrogen generation, in order to meet the requirements of portable applications. The system was run in batch mode. The core of their system consisted of a catalytic reactor for the hydrolysis of NaBH_4 . Inside the reactor, magnetic elements were able to hold a non-noble, inexpensive magnetic catalyst. They used commercial cylindrical magnets made up of sintered neodymium iron boron. The use of internal magnets created a magnetic field to which the catalytic material was attracted preventing any entrapment caused by the turbulent two-phase solution running through the reactor. The authors charged the solution tank with a fixed volume of NaBH_4 solution. This solution was replaced with a new one when the NaBH_4 concentration dropped below $\sim 1\%$ *w/v*. Their reaction test was usually conducted at ambient temperature and at atmospheric pressure. The performance of the magnetic-containment reactor was measured in a test-rig, showing a continuous hydrogen flowrate of 25 mL/min with an overall system efficiency of about 90%.

Gislon et al., designed, tested and optimized a system for the controlled production of hydrogen, which was able to deliver hydrogen flows in the 0.1–0.3 L/min range for more than 20 h. Such hydrogen flow is suitable to power a 10–30 W fuel cell unit [98]. Their system was based on the hydrolysis of catalyzed solid-state NaBH_4 . Through their experimental activities, the authors aimed to identify the most appropriate configuration in order to diffuse water homogeneously into NaBH_4 powder and to provide the necessary operating parameters for a system able to generate a controlled on-demand hydrogen flow. They tested three reactor designs consisting of two concentric cylinders and an internal water diffuser and cartridge case, with the cartridge itself being filled with NaBH_4 . In their system, the water was pumped from the bottom. They varied the water diffuser system in configurations for each reactor. The aim of this method was to uniformly distribute small quantities of water inside the powder using an electronically controlled pump. The upper flange collected the produced hydrogen, which was subsequently filtered and monitored. The set of the experimental conditions such as reactor layout, input reactant and input flow, reactor temperature, water temperature, and sample mass was monitored. For temperature monitoring, a thermocouple was inserted into the reaction chamber.

Ferreira et al., performed H_2 generation experiments at room temperature in three batch reactors with different internal volumes and bottom geometries, emphasizing the importance of considering the influence of reactor bottom geometry on the optimization of water handling through NaBH_4 hydrolysis studies [99]. One of their reactors was 646 cm^3 with flat bottom shape; another was 229 cm^3 , also with flat bottom geometry; and the last one investigated was 229 cm^3 , with a conical bottom shape. The mixture of NaBH_4 and catalyst was stored inside the batch reactors and liquid water was rapidly added by means of a syringe with a long needle, ensuring the water was delivered very close to the powder mixture. The temperature of the reactor was monitored. Their results show the conical

bottom geometry significantly increased both the hydrogen yield and generation rates, and decreased the induction time, during the solid-state NaBH_4 hydrolysis experiments. They gave a plausible explanation that the reactor with a conical bottom shape enhances the contact between the catalyst and NaBH_4 powders and the injected distilled water.

Sousat et al. [93] conducted experiments at atmospheric pressure in a batch tubular reactor. Their system was run at different temperatures and was equipped with a thermocouple and a thermostatic circulation water bath. The purpose was to construct kinetic models in order to describe the behavior of the NaBH_4 hydrolysis reaction. They used their model to simulate a pilot scale reactor and to validate the kinetic model. Their reactor was made out of stainless steel and could operate up to 60 bars. The total volume for the reaction and storage region was 21 dm³.

Marchionni et al. [100] aimed to feed a 2 kW scale PEMFC stack by developing an apparatus for H_2 generation via NaBH_4 hydrolysis. The reactor comprised a cylindrical stainless-steel chamber. A replaceable head piece with a stainless-steel rod whose vertical movement was controlled by a stepper motor was located on the top. The warm water was circulated inside the reactor. The initial temperature of the solution was controlled by a copper coil. The seal of the reactor was tested prior to any experiments using H_2 up to a pressure of 10 bars. Throughout all of the experiments, the catalyst was totally immersed in the solution. At 5 bar pressure, the catalyst was capable of generating up to 35 L H_2 /(min \times g_{catalyst}).

Lee et al. [101] generated hydrogen from solid-state NaBH_4 using a HCl solution to circumvent the use of a catalyst. The aim was to address the need for a portable and stable hydrogen supply system for integration with a fuel cell. Their hydrogen supply system successfully provided a stable hydrogen supply to the fuel cell, allowing the 100 W fuel cell to operate reliably with an electric load of 0–6 A.

Minkina et al. [102] used a solution of sodium borohydride in the presence of Al_2O_3 -supported Pt, Pd, Rh, and Ni catalysts to create a hydrogen generator that ran on a circulation system.

They tested a hydrogen generator coupled with a PEMFC Nexa™ Power module from Ballard. The most important parameters, such as the initial working conditions and variation in temperature, as well as the concentration of the sodium borohydride and metaborate, catalytic activity, and removal of the NaBO_2 by-product were analyzed. They reported that the circulation process significantly improved the mass transport between the solution and the catalytic surface. They found the kinetic constraints imposed by the rates of heterogeneous reactions, which are governed by temperature and catalyst characteristics, were unaffected by this process. For the operation of the PEMFC Nexa™ Power module from Ballard, a rate of 1.5 Nm³/h hydrogen gas generation with an average hydrogen yield of about 98% indicates satisfactory catalytic efficiency.

Cento et al., manufactured a stainless-steel reactor comprising a thermostatic bath, a reaction chamber in which the NaBH_4 and the $\text{Ni}(\text{CH}_3\text{COO})_2$ catalyst or $\text{Fe}_2(\text{SO}_4)_3$ are placed, a water inlet, and a hydrogen outlet [103]. The authors reported that the hydrogen release rate exhibited a plateau-like pattern during the reaction because it was limited by the solubility of NaBH_4 in water.

Özkan et al., combined experimental data with a Box–Wilson statistical experimental design technique to optimize the reaction temperature [104,105]. Their experiments were carried out under different operating conditions and HCl concentrations to determine the maximum amount of hydrogen, which they found to be about 3.7 M HCl and 430K.

Nunes et al., presented an innovative portable batch mini-reactor for hydrogen generation via catalytic hydrolysis of NaBH_4 for small portable fuel cells [106]. The new portable mini-reactor had an ovoid geometry and was constructed using AISI 316 L stainless-steel with a 9 cm³ internal volume. A Ni-Ru catalyst was used in this reaction [107,108]. This mini-reactor generated 0.98 35 L H_2 /(min \times g_{catalyst}). The produced hydrogen generated 1.4 V, which was enough to charge a smartphone for 5 min. [109].

So far, the methods and reactors used for carrying out the NaBH_4 hydrolysis reaction are under development [110–114]. There is no conclusive approach. Each approach has its advantages and drawbacks. There are several factors to understand, and further explorations could advance the development of reactors and portable reactors for the generation of hydrogen through hydrolysis of NaBH_4 .

6. Conclusions

Hydrogen has a number of issues in terms of production, transportation, and storage, as well as in both direct and fuel-cell combustion. Great efforts have been made in recent years to create appropriate materials with high gravimetric and volumetric density for hydrogen storage. This short review deals with hydrogen generation efforts utilizing hydrolysis of NaBH_4 and catalysts, from its inception to the present. Despite the fact that it is no longer approved for vehicle usage, NaBH_4 nevertheless has potential to be used in other applications. The collected information shows that catalysts have received a lot of attention, while the other elements have been passed over. Investigations reported in the literature have indicated, however, that there is not a substantial reason to dwell on the catalyst. Setbacks due to precipitation of NaBO_2 , which would block the active sites of the catalysts, and the formation of by-products are mentioned in the literature as potential issues, due to their tendency to cause clogging; these issues have not been satisfactorily resolved. In addition to these, the concentration of borate ions in the aqueous product solution (which is basic), will increase, meaning that the initially moderate rate of the reaction will quickly slow, and eventually stop. Although sodium borohydride has a variety of features that make it a potentially excellent source of hydrogen, it does have some obviously drawbacks; for example, the hydrolysis reaction requires more water than is needed stoichiometry in order to keep the NaBH_4 in solution. This excess water leads to a massive decrease in the gravimetric capacity. One advantage is that, with water, the reaction spontaneously generates hydrogen. However, the method for supplying and distributing water within the reactor or system in order to develop the reaction requires further detailed and systematic studies. To demonstrate the technological potential of hydrogen production utilizing sodium borohydride hydrolysis and to move towards practical applications with higher productivity, a systematic boost is required. The pathway of NaBH_4 hydrolysis must be greatly improved. The concentrations of NaBH_4 and any catalysts, as well as the form in which they are introduced into the reaction, the changes in temperature throughout the hydrogen generation process, and the amount of heat released by the reaction are all significant factors influencing the reaction rate. In addition, the impact of the initial temperature is another crucial factor, which impacts on the whole hydrolysis process.

Funding: This review paper received no external funding.

Data Availability Statement: Not applicable.

Acknowledgments: I would like to thank my colleagues (*alphabetical list by last name*) Sebastian Brad, Stanica Enache, Monica Mihalcea, Cristian Pupaza, and Mihai Vijulie for invigorating dialogue during the time I was working on this review.

Conflicts of Interest: The author declares no conflict of interest.

References

1. NIST Chemistry WebBook. Available online: <https://webbook.nist.gov/chemistry/> (accessed on 24 January 2022).
2. U.S. Department of Energy, Office of Basic Energy Sciences. Basic Research Needs for the Hydrogen Economy, Report. 2003. Available online: <http://www.sc.doe.gov/bes/hydrogen.pdf> (accessed on 24 January 2022).
3. Ross, D.K. Hydrogen storage: The major technological barrier to the development of hydrogen fuel cell cars. *Vacuum* **2006**, *80*, 1084–1089. <https://doi.org/10.1016/j.vacuum.2006.03.030>.
4. Maestre, V.M.; Ortiz, A.; Ortiz, I. Challenges and prospects of renewable hydrogen-based strategies for full decarbonization of stationary power applications. *Renew. Sustain. Energy Rev.* **2021**, *152*, 111628. <https://doi.org/10.1016/j.rser.2021.111628>.

5. Egeland-Eriksen, T.; Hajizadeh, A.; Sartori, S. Hydrogen-based systems for integration of renewable energy in power systems: Achievements and perspectives. *Int. J. Hydrogen Energy* **2021**, *46*, 31963–31983. <https://doi.org/10.1016/j.ijhydene.2021.06.218>.
6. *Comprehensive Inorganic Chemistry-II*; Reedijk, J., Poeppelemeier, K., Eds.; Elsevier: Amsterdam, The Netherlands, 2013; ISBN: 9780080977744
7. Mao, J.; Gregory, D.H. Recent Advances in the Use of Sodium Borohydride as a Solid State Hydrogen Store. *Energies* **2015**, *8*, 430–453. <https://doi.org/10.3390/en8010430>
8. Abdelhamid H.N. A review on hydrogen generation from the hydrolysis of sodium borohydride. *Int. J. Hydrogen Energy* **2021**, *46*, 726–765. <https://doi.org/10.1016/j.ijhydene.2020.09.186>.
9. Schlesinger, H.I.; Brown, H.C.; Sheft, I.; Ritter, D.M. Addition compounds of alkali metal hydrides sodium trimethoxyborohydride and related compounds. *J. Am. Chem. Soc.* **1953**, *75*, 192–195.
10. U.S. Department of Energy Hydrogen Program. Go/no-go recommendation for sodium borohydride for on-board vehicular hydrogen storage. *Independ. Rev.* **2007**, *150*, 1–21.
11. Schlesinger, H.I.; Brown, H.C.; Finholt, A.E. The Preparation of Sodium Borohydride by the High Temperature Reaction of Sodium Hydride with Borate Esters. *J. Am. Chem. Soc.* **1953**, *75*, 205–209. <https://doi.org/10.1021/ja01097a054>.
12. Schlesinger, H.I.; Brown, H.C.; Abraham, B.; Bond, A.C.; Davidson, N.; Finholt, A.E.; Gilbreath, J.R.; Hoekstra, H.; Horvitz, L.; Hyde, E.K.; et al. New Developments in the Chemistry of Diborane and the Borohydrides. I. General Summary. *J. Am. Chem. Soc.* **1953**, *75*, 186–190. <https://doi.org/10.1021/ja01097a049>.
13. Broja, G.; Schlabacher, W. Process for the Production of Alkali Metal Borohydrides. U.S. Patent US3259474A, 5 July 1966.
14. Schlesinger, H.I.; Brown, H.C.; Hoekstra, H.R.; Rapp, L.R. Reactions of diborane with alkali metal hydrides and their addition compounds. New syntheses of borohydrides. Sodium and potassium borohydrides. *J. Am. Chem. Soc.* **1953**, *75*, 199–204. <https://doi.org/10.1021/Ja01097A053>.
15. Umeda, H.; Sasaki, A.; Takahashi, K.; Haga, K.; Yasushi Takasaki, Y.; Shibayama, A. Recovery and Concentration of Precious Metals from Strong Acidic Wastewater. *Mater. Trans.* **2011**, *52*, 1462–1470. <https://doi.org/10.2320/matertrans.M2010432>.
16. *Handbook of Fuel Cells: Fundamentals, Technology, Applications*; Vielstich, W., Lamm, A., Hubert, A., Eds.; John Wiley & Sons, Inc.: Hoboken, NJ, USA 2003. ISBN: 978-0-471-49926-8.
17. Schlesinger, H.I.; Brown, H.C.; Finholt, A.E.; Gilbreath, J.R.; Hoekstra, H.R.; Hyde, E.K. Sodium Borohydride, Its Hydrolysis and its Use as a Reducing Agent and in the Generation of Hydrogen. *J. Am. Chem. Soc.* **1953**, *75*, 215–219. <https://doi.org/10.1021/ja01097a057>.
18. Richardson, B.S.; Birdwell, J.F.; Pin, F.G.; Jansen, J.F.; Lind, R.F. Sodium borohydride based hybrid power system. *J. Power Sources* **2005**, *145*, 21–29. <https://doi.org/10.1016/j.jpowsour.2004.12.057>.
19. Duggan, P.J.; Johnson, A.A.; Rogers, R.L. Chemical reaction hazards associated with the use of sodium borohydride. In *Institution of Chemical Engineers Symposium Series*; IChemE Symposium Series no. 134—Hazards; Hemisphere Publishing Corporation: London, UK, 1994; Volume 12, pp. 553–561.
20. Cook, M.M.; Lander, J.A. Use of Sodium Borohydride to Control Heavy Metal Discharge in the Photographic Industry. *J. Appl. Photogr. Eng.* **1979**, *5*, 144–147.
21. Stevens, M.R.; Pirnazari, M.; Saavedra, F. *Removal of Silver from Photographic Solutions*; Pawlowski, L., Verdier, A.J., Lacy, W.J., Eds.; Studies in Environmental Science; Elsevier: Amsterdam, The Netherlands, 1984; Volume 23, pp. 525–534. [https://doi.org/10.1016/S0166-1116\(08\)71258-5](https://doi.org/10.1016/S0166-1116(08)71258-5).
22. Tang, L.C. Stabilization of Paper Through Sodium Borohydride Treatment. Chapter 24—Historic Textile and Paper Materials. *Adv. Chem.* **1986**, *212*, 427–441. <https://doi.org/10.1021/ba-1986-0212.ch024>.
23. Westbroek, P. Chapter 7—Advantages of electrocatalytic reactions in textile applications: Example—Electrocatalytic oxidation of sodium dithionite at a phthalocyanine and porphyrin cobalt(II)-modified gold electrode. In *Analytical Electrochemistry in Textiles*; Westbroek, P., Priniotakis, G., Kiekens, P., Eds.; Woodhead Publishing Series in Textile; Elsevier: Amsterdam, The Netherlands, 2007; pp. 198–211.
24. Source of hydrogen & other borohydrides; bleacher of wood pulp; blowing agent for plastics. In *Patty's Industrial Hygiene and Toxicology*; Clayton, G.D., Clayton, F.E., Eds.; John Wiley & Sons: Hoboken, NJ, USA, 1991; 1981–1982, (2A, 2B, 2C), 2995.
25. Soyeon, C. Foxing on Paper: A Literature Review. *J. Am. Inst. Conserv.* **2020**, *46*, 137–152. <https://doi.org/10.1179/019713607806112378>.
26. Yilmazer, D.; Kanik, M. Bleaching of Wool with Sodium Borohydride. *J. Eng. Fibers Fabr.* **2009**, *4*, 45–50. <https://doi.org/10.1177/155892500900400305>.
27. Li, Q.; Zhang, H.; Li, C.; Xu, P. Stereoselective Synthesis of (–)-Chloramphenicol, (+)-Thiamphenicol and (+)-Sphinganine via Chiral Tricyclic Iminolactone. *Chin. J. Chem.* **2013**, *31*, 149–153. <https://doi.org/10.1002/cjoc.201201093>.
28. Odinkov, V.N.; Spivak, A.Y.; Emelyanova, G.A.; Mallyabaeva, M.I.; Nazarova, O.V.; Dzhemilev, U.M. Synthesis of α -tocopherol (vitamin E), vitamin K1-chromanol, and their analogs in the presence of aluminosilicate catalysts Tseokar-10 and Pentasil. *Arkhivov. Org. Chem.* **2003**, *13*, 101–118. <https://doi.org/10.3998/ark.5550190.0004.d11>. January, 2022.
29. De Keukeleire, D. Fundamentals of beer and hop chemistry. *Quím. Nova* **2000**, *23*, 108–112. <https://doi.org/10.1590/S0100-40422000000100019>.
30. Chaikin, S.W.; Brown, W.G. Reduction of Aldehydes, Ketones and Acid Chlorides by Sodium Borohydride. *J. Am. Chem. Soc.* **1949**, *71*, 122–125. <https://doi.org/10.1021/ja01169a033>.

31. O'Neil, M.J. *The Merck Index—An Encyclopedia of Chemicals, Drugs, and Biologicals*, 13th ed.; The Royal Society of Chemistry: London, UK, 2001; 1537.
32. Viswanathan, B. *Chapter 10—Hydrogen Storage. Energy Sources*; Viswanathan, B., Ed.; Elsevier: Amsterdam, The Netherlands, 2017; pp. 185–212. <https://doi.org/10.1016/B978-0-444-56353-8.00010-1>.
33. Abanades, S.; Flamant, G. Thermochemical hydrogen production from a two-step solar-driven water-splitting cycle based on cerium oxides. *Sol. Energy* **2006**, *80*, 1611–1623. <https://doi.org/10.1016/j.solener.2005.12.005>.
34. Dincer, I.; Rosen, M.A. *Chapter 17—Exergy Analysis of Hydrogen Production Systems*; Elsevier: Amsterdam, The Netherlands, 2013; pp. 347–362.
35. Ma, J.; Choudhury, N.A.; Sahai, Y. A comprehensive review of direct borohydride fuel cells. *Renew. Sustain. Energy Rev.* **2001**, *14*, 183–199. <https://doi.org/10.1016/j.rser.2009.08.002>.
36. Sundén, B. *Chapter 3—Hydrogen, Hydrogen, Batteries and Fuel Cells*; Academic Press: Cambridge, MA, USA, 2001; pp. 37–55.
37. Filinchuk, Y.; Hagemann, H. Structure and Properties of NaBH₄·2H₂O and NaBH₄. *Eur. J. Inorg. Chem.* **2008**, *20*, 3127–3133. <https://doi.org/10.1002/ejic.200800053>.
38. Diamond—Crystal and Molecular Structure Visualization, Crystal Impact—Dr. H. Putz & Dr. K. Brandenburg GbR, Kreuzherrenstr. 102, 53227 Bonn, Germany. Available online: <https://www.crystalimpact.de/diamond> (accessed on 24 January 2022).
39. Johnston, H.L.; Hallett, N.C. Low Temperature Heat Capacities of Inorganic Solids. XIV. Heat Capacity of Sodium Borohydride from 15–300 °K. *J. Am. Chem. Soc.* **1953**, *75*, 1467–1468. <https://doi.org/10.1021/ja01102a056>.
40. Stockmayer, W.H.; Stephenson, C.C. The Nature of the Gradual Transition in Sodium Borohydride. *J. Chem. Phys.* **1953**, *21*, 1311–1312. <https://doi.org/10.1063/1.1699207>.
41. Abrahams, S.C.; Kalnajs, J. The Lattice Constants of the Alkali Borohydrides and the Low-Temperature Phase of Sodium Borohydride. *J. Chem. Phys.* **1954**, *22*, 434. <https://doi.org/10.1063/1.1740085>.
42. Stockmayer, W.H.; Rice, D.W.; Stephenson, C.C. Thermodynamic Properties of Sodium Borohydride and Aqueous Borohydride Ion. *J. Am. Chem. Soc.* **1955**, *77*, 1980–1983. <https://doi.org/10.1021/ja01612a082>.
43. Fischer, P.; Züttel, A. Order-Disorder Phase Transition in NaBD₄. *Mater. Sci. Forum* **2004**, *443–444*, 287–290. <https://doi.org/10.4028/www.scientific.net/MSF.443-444.287>.
44. Filinchuk, Y.; Talyzin, A.V.; Chernyshov, D.; Dmitriev, V. High-pressure phase of NaBH₄: Crystal structure from synchrotron powder diffraction data. *Phys. Rev. B* **2007**, *76*, 092104. <https://doi.org/10.1103/PhysRevB.76.092104>.
45. Kim, E.; Kumar, R.; Weck, P.F.; Cornelius, A.L.; Nicol, M.; Vogel, S.C.; Zhang, J.; Hartl, M.; Stowe, A.C.; Daemen, L.; et al. Pressure-driven phase transitions in NaBH₄: Theory and experiments. *Phys. Rev. B* **2007**, *111*, 13873–13876. <https://doi.org/10.1021/jp709840w>.
46. Kojima, Y.; Haga, T. Recycling process of sodium metaborate to sodium borohydride. *Int. J. Hydrog. Energy* **2003**, *28*, 989–993. [https://doi.org/10.1016/S0360-3199\(02\)00173-8](https://doi.org/10.1016/S0360-3199(02)00173-8).
47. Zhang, J.; Delgass, W.; Fisher, T.; Gore, J. Kinetics of Ru catalyzed sodium borohydride hydrolysis. *J. Power Sources* **2007**, *164*, 772–781. <https://doi.org/10.1016/j.jpowsour.2006.11.002>.
48. Wee, J.H.; Lee, K.Y.; Kim, S.H. Sodium borohydride as the hydrogen supplier for proton exchange membrane fuel cell systems. *Fuel Process. Technol.* **2006**, *87*, 811–819. <https://doi.org/10.1016/j.fuproc.2006.05.001>.
49. Maier Chas. G.; Kelley, K.K.; An equation for the representation of high-temperature of high heat content data. *J. Am. Chem. Soc.* **1932**, *54*, 3243–3246. <https://doi.org/10.1021/ja01347a029>.
50. *Thermophysical Properties of Materials*; Grimvall, G., Ed.; Elsevier Science B.V.: Amsterdam, The Netherlands, 1999. ISBN 9780444827944. <https://doi.org/10.1016/B978-0-444-82794-4.50034-6>.
51. Lide, D.R.; Kehiaian, H.V. *CRC Handbook of Thermophysical and Thermochemical Data*; CRC: Boca Raton, FL, USA, 1994.
52. Mochalov, K.N.; Khain, V.S.; Gil'manshin, G.G. A generalized scheme for the hydrolysis of the borohydride ion and diborane. *Dokl. Akad. Nauk SSSR* **1965**, *162*, 613–616.
53. Demirci, U.B.; Mielea, P. Cobalt-based catalysts for the hydrolysis of NaBH₄ and NH₃BH₃. *Phys. Chem. Chem. Phys.* **2014**, *16*, 6872–6885. <https://doi.org/10.1039/C4CP00250D>.
54. Seven, F.; Sahiner, N. Enhanced catalytic performance in hydrogen generation from NaBH₄ hydrolysis by super porous cryogel supported Co and Ni catalysts. *J. Power Sources* **2014**, *272*, 128–136. <https://doi.org/10.1016/j.jpowsour.2014.08.047>.
55. Netskina, O.V.; Tayban, E.S.; Rogov, V.A.; Ozerova, A.M.; Mukha, S.A.; Simagina, V.I.; Komova, O.V. Solid-state NaBH₄ composites for hydrogen generation: Catalytic activity of nickel and cobalt catalysts. *Int. J. Hydrogen Energy* **2021**, *46*, 5459–5471. <https://doi.org/10.1016/j.ijhydene.2020.11.078>.
56. Brown, H.C.; Subba, R.B.C. A New Powerful Reducing Agent—Sodium Borohydride in the Presence of Aluminum Chloride and Other Polyvalent Metal Halides. *J. Am. Chem. Soc.* **1956**, *78*, 2582–2588. <https://doi.org/10.1021/ja01592a070>.
57. Jung, S.C.; Nahm, S.W.; Jung, H.Y.; Park, Y.K.; Seo, S.G.; Kim, S.C. Preparations of Platinum Nanoparticles and Their Catalytic Performances. *J. Nanosci. Nanotechnol.* **2015**, *15*, 5461–5465. <https://doi.org/10.1166/jnn.2015.10394>.
58. Soltani, M.; Zabihi, M. Hydrogen generation by catalytic hydrolysis of sodium borohydride using the nano-bimetallic catalysts supported on the core-shell magnetic nanocomposite of activated carbon. *Int. J. Hydrogen Energy* **2020**, *45*, 12331–12346. <https://doi.org/10.1016/j.ijhydene.2020.02.203>.
59. Brown, C.A. Catalytic hydrogenation. V. Reaction of sodium borohydride with aqueous nickel salts. P-1 nickel boride, a convenient, highly active nickel hydrogenation catalyst. *J. Org. Chem.* **1970**, *35*, 1900–1904. <https://doi.org/10.1021/jo00831a039>.

60. Amendola, S.C.; Binder, M.; Kelly, M.T.; Petillo, P.J.; Sharp-Goldman, S.L. A Novel Catalytic Process for Generating Hydrogen Gas from Aqueous Borohydride Solutions. In *Advances in Hydrogen Energy*; Padró, C.E.G., Lau, F., Eds.; Springer, Boston, MA, USA, 2002. https://doi.org/10.1007/0-306-46922-7_6.
61. Paksoy, A.; Kurtoğlu, S.F.; Dizaji, A.K.; Altıntaş, Z.; Khoshsima, S.; Uzun, A.; Balci, Ö. Nanocrystalline cobalt–nickel–boron (metal boride) catalysts for efficient hydrogen production from the hydrolysis of sodium borohydride. *Int. J. Hydrogen Energy* **2021**, *46*, 7974–7988. <https://doi.org/10.1016/j.ijhydene.2020.12.017>.
62. Damjanović, L.; Majchrzak, M.; Bennici, S.; Auroux, A. Determination of the heat evolved during sodium borohydride hydrolysis catalyzed by Co_3O_4 . *Int. J. Hydrogen Energy* **2011**, *36*, 1991–1997. <https://doi.org/10.1016/j.ijhydene.2010.11.041>.
63. Fernandes, R.; Patel, N.; Miotello, A.; Jaiswal, R.; Kothari, D.C. Dehydrogenation of Ammonia Borane with transition metal-doped Co–B alloy catalysts. *Int. J. Hydrogen Energy* **2012**, *37*, 2397–2406. <https://doi.org/10.1016/j.ijhydene.2011.10.119>.
64. Yang, C.C.; Chen, M.S.; Chen, Y.W. Hydrogen generation by hydrolysis of sodium borohydride on CoB/SiO₂ catalyst. *Int. J. Hydrogen Energy* **2011**, *36*, 1418–1423. <https://doi.org/10.1016/j.ijhydene.2010.11.006>.
65. Sahiner, N.; Ozay, O.; Inger, E.; Aktas, N. Superabsorbent hydrogels for cobalt nanoparticle synthesis and hydrogen production from hydrolysis of sodium boron hydride. *Appl. Catal. B Environ.* **2011**, *102*, 201–206. <https://doi.org/10.1016/j.apcatb.2010.11.042>.
66. Chen, B.; Chen, S.; Bandal, H.A.; Appiah-Ntiamoah, R.; Jadhav, A.R.; Kim, H. Cobalt nanoparticles supported on magnetic core-shell structured carbon as a highly efficient catalyst for hydrogen generation from NaBH_4 hydrolysis. *Int. J. Hydrogen Energy* **2018**, *43*, 9296–9306. <https://doi.org/10.1016/j.ijhydene.2018.03.193>.
67. Ma, H.; Ji, W.; Zhao, J.; Liang, J.; Chen, J. Preparation, characterization and catalytic NaBH_4 hydrolysis of Co-B hollow spheres. *J. Alloys Compd.* **2009**, *474*, 584–589. <https://doi.org/10.1016/j.jallcom.2008.07.005>.
68. Sun, L.; Meng, Y.; Kong, X.; Ge, H.; Chen, X.; Ding, C.; Yang, H.; Li, D.; Gao, X.; Dou, J. Novel high dispersion and high stability cobalt-inlaid carbon sphere catalyst for hydrogen generation from the hydrolysis of sodium borohydride. *Fuel* **2022**, *31*, 122276. <https://doi.org/10.1016/j.fuel.2021.122276>.
69. Demirci, U.B.; Miele, P. Reaction mechanisms of the hydrolysis of sodium borohydride: A discussion focusing on cobalt-based catalysts. *C. R. Chim.* **2014**, *17*, 707–716. <https://doi.org/10.1016/j.crci.2014.01.012>.
70. Hua, D.; Hanxi, Y.; Xinping, A.; Chuansin, C. Hydrogen production from catalytic hydrolysis of sodium borohydride solution using nickel boride catalyst. *Int. J. Hydrogen Energy* **2003**, *28*, 1095–1100. [https://doi.org/10.1016/S0360-3199\(02\)00235-5](https://doi.org/10.1016/S0360-3199(02)00235-5).
71. Tignol, P.; Demirci, U.B. Nickel-based catalysts for hydrogen evolution by hydrolysis of sodium borohydride: From structured nickel hydrazine nitrate complexes to reduced counterparts. *Int. J. Hydrogen Energy* **2019**, *44*, 14207–14216. <https://doi.org/10.1016/j.ijhydene.2018.10.147>.
72. Ghodke, N.P.; Rayaprol, S.; Bhoraskar, S.V.; Mathe, V.L. Catalytic hydrolysis of sodium borohydride solution for hydrogen production using thermal plasma synthesized nickel nanoparticles. *Int. J. Hydrogen Energy* **2020**, *45*, 16591–16605. <https://doi.org/10.1016/j.ijhydene.2020.04.143>.
73. Kaufman, C.M.; Sen, B. Hydrogen generation by hydrolysis of sodium tetrahydroborate: Effects of acids and transition metals and their salts. *J. Chem. Soc. Dalton Trans.* **1985**, 307–313. <https://doi.org/10.1039/DT9850000307>.
74. Wei, Y.; Wang, Y.; Wei, L.; Zhao, X.; Zhou, X.; Liu, H. Highly efficient and reactivated electrocatalyst of ruthenium electrodeposited on nickel foam for hydrogen evolution from NaBH_4 alkaline solution. *Int. J. Hydrogen Energy* **2018**, *43*, 592–600. <https://doi.org/10.1016/j.ijhydene.2017.11.010>.
75. Liang, Z.; Li, Q.; Li, F.; Zhao, S.; Xia, X. Hydrogen generation from hydrolysis of NaBH_4 based on high stable NiB/NiFe₂O₄ catalyst. *Int. J. Hydrogen Energy* **2017**, *42*, 3971–3980. <https://doi.org/10.1016/j.ijhydene.2016.10.115>.
76. Amendola, S.C.; Sharp-Goldman, S.L.; Janjua, M.S.; Spencer, N.C.; Kelly, M.T.; Petillo, P.J.; Binder, M. A safe, portable, hydrogen gas generator using aqueous borohydride solution and Ru catalyst. *Int. J. Hydrogen Energy* **2000**, *25*, 969–975. [https://doi.org/10.1016/S0360-3199\(00\)00021-5](https://doi.org/10.1016/S0360-3199(00)00021-5).
77. Brown, H.C.; Brown, C.A. Reaction of Sodium Borohydride with Platinum Metal Salts in the Presence of Decolorizing Carbon-A Supported Platinum Catalyst of Markedly Enhanced Activity for Hydrogenations. *J. Am. Chem. Soc.* **1962**, *84*, 2827–2827. <https://doi.org/10.1021/ja00873a037>.
78. Liu, Z.; Guo, B.; Chan, S.H.; Tang, E.H.; Hong, L. Pt and Ru dispersed on LiCoO₂ for hydrogen generation from sodium borohydride solutions. *J. Power Sources* **2008**, *176*, 306–311. <https://doi.org/10.1016/j.jpowsour.2007.09.114>.
79. Chen, Y.H.; Pan, C.Y. Effect of various Co–B catalyst synthesis conditions on catalyst surface morphology and NaBH_4 hydrolysis reaction kinetic parameters. *Int. J. Hydrogen Energy* **2014**, *39*, 1648–1663. <https://doi.org/10.1016/j.ijhydene.2013.11.067>.
80. Liang, Y.; Dai, H.B.; Ma, L.P.; Wang, P.; Cheng, H.M. Hydrogen generation from sodium borohydride solution using a ruthenium supported on graphite catalyst. *Int. J. Hydrogen Energy* **2010**, *35*, 3023–3028. <https://doi.org/10.1016/j.ijhydene.2009.07.008>.
81. Senliang, X.; Xiaojun, W.; Dan, W.; Xingtao, H.; Shixue, Z.; Hao, Y. Efficient Hydrogen Generation from Hydrolysis of Sodium Borohydride in Seawater Catalyzed by Polyoxometalate Supported on Activated Carbon. *Front. Chem.* **2020**, *8*, 676. <https://doi.org/10.3389/fchem.2020.00676>.
82. Jadhav, A.R.; Bandal, H.A.; Kim, H. NiCo₂O₄ hollow sphere as an efficient catalyst for hydrogen generation by NaBH_4 hydrolysis. *Mater. Lett.* **2017**, *198*, 50–53. <https://doi.org/10.1016/j.matlet.2017.03.161>.
83. Bandal, H.A.; Jadhav, A.R.; Kim, H. Cobalt impregnated magnetite-multiwalled carbon nanotube nanocomposite as magnetically separable efficient catalyst for hydrogen generation by NaBH_4 hydrolysis. *J. Alloys Compd.* **2017**, *699*, 1057–1067. <https://doi.org/10.1016/j.jallcom.2016.12.428>.

84. Kim, C.; Lee, S.S.; Li, W.; Fortner, J.D. Towards optimizing cobalt based metal oxide nanocrystals for hydrogen generation via NaBH_4 hydrolysis. *Appl. Catal. A Gen.* **2020**, *589*, 117303. <https://doi.org/10.1016/j.apcata.2019.117303>.
85. Tiri, R.N.E.; Gulbagca, F.; Aygun, A.; Cherif, A.; Sen, F. Biosynthesis of Ag–Pt bimetallic nanoparticles using propolis extract: Antibacterial effects and catalytic activity on NaBH_4 hydrolysis. *Environ. Res.* **2022**, *206*, 112622. <https://doi.org/10.1016/j.envres.2021.112622>.
86. Zhou, S.; Yang, Y.; Zhang, W.; Rao, X.; Yan, P.; Isimjan, T.T.; Yang, X. Structure-regulated Ru particles decorated P-vacancy-rich CoP as a highly active and durable catalyst for NaBH_4 hydrolysis. *J. Colloid Interface Sci.* **2021**, *591*, 221–228. <https://doi.org/10.1016/j.jcis.2021.02.009>.
87. Wang, J.; Ke, D.; Yuan Li, Y.; Zhang, H.; Wang, C.; Zhao, X.; Yuan, Y.; Han, S. Efficient hydrolysis of alkaline sodium borohydride catalyzed by cobalt nanoparticles supported on three-dimensional graphene oxide. *Mater. Res. Bull.* **2017**, *95*, 204–210. <https://doi.org/10.1016/j.materresbull.2017.07.039>.
88. İzgi, M.S.; Baytar, O.; Şahin, Ö.; Kazıcı, H.Ç. CeO_2 supported multimetallic nano materials as an efficient catalyst for hydrogen generation from the hydrolysis of NaBH_4 . *Int. J. Hydrogen Energy* **2020**, *45*, 34857–34866. <https://doi.org/10.1016/j.ijhydene.2020.04.034>.
89. Liao, J.; Huang, H. Magnetic sensitive Hericium erinaceus residue chitin/Cu hydrogel nanocomposites for H_2 generation by catalyzing NaBH_4 hydrolysis. *Carbohydr. Polym.* **2020**, *229*, 115426. <https://doi.org/10.1016/j.carbpol.2019.115426>.
90. Prasad, D.; Patil, K.N.; Sandhya, N.; Chaitra, C.R.; Bhanushali, J.T.; Samal, A.K.; Keri, R.S.; Jadhav, A.H.; Nagaraja, B.M. Highly efficient hydrogen production by hydrolysis of NaBH_4 using eminently competent recyclable Fe_2O_3 decorated oxidized MWCNTs robust catalyst. *Appl. Surf. Sci.* **2019**, *489*, 538–551. <https://doi.org/10.1016/j.apsusc.2019.06.041>.
91. Zahmakiran, M.; Özkar, S. Zeolite-Confined Ruthenium(0) Nanoclusters Catalyst: Record Catalytic Activity, Reusability, and Lifetime in Hydrogen Generation from the Hydrolysis of Sodium Borohydride. *Langmuir* **2009**, *25*, 2667–2678. <https://doi.org/10.1021/la803391c>.
92. Hung, A.J.; Tsai, S.F.; Hsu, Y.Y.; Ku, J.R.; Chen, Y.H.; Yu, C.C. Kinetics of sodium borohydride hydrolysis reaction for hydrogen generation. *Int. J. Hydrogen Energy* **2008**, *33*, 6205–6215. <https://doi.org/10.1016/j.ijhydene.2008.07.109>.
93. Sousa, T.; Fernandes, V.R.; Pinto, P.J.R.; Slavkov, Y.; Bosukov, L.; Rangel, C.M. A sodium borohydride hydrogen generation reactor for stationary applications: Experimental and reactor simulation studies. *Chem. Eng. Sci.* **2012**, *84*, 70–79. <https://doi.org/10.1016/j.ces.2012.08.001>.
94. Brewer, J.H.; Heer, A.A.; McLaughlin, C.B. The use of sodium borohydride for producing hydrogen in an anaerobe jar. *Appl. Microbiol.* **1955**, *3*, 136. <https://doi.org/10.1128/am.3.3.136-136.1955>.
95. Zhang, J.; Zheng, Y.; Gore, J.P.; Fisher, T.S. 1kWe sodium borohydride hydrogen generation system: Part I: Experimental study. *J. Power Sources* **2007**, *165*, 844–853. <https://doi.org/10.1016/j.jpowsour.2006.12.055>.
96. Zhang, J.; Zheng, Y.; Gore, J.P.; Mudawar, I.; Fisher, T.S. 1kWe sodium borohydride hydrogen generation system: Part II: Reactor modeling. *J. Power Sources* **2007**, *170*, 150–159. <https://doi.org/10.1016/j.jpowsour.2007.03.025>.
97. Oronzio, R.; Monteleone, G.; Pozio, A.; De Francesco, M.; Galli, S. New reactor design for catalytic sodium borohydride hydrolysis. *Int. J. Hydrogen Energy* **2009**, *34*, 4555–4560. <https://doi.org/10.1016/j.ijhydene.2009.01.056>.
98. Gislou, P.; Monteleone, G.; Prosini, P.P. Hydrogen production from solid sodium borohydride. *Int. J. Hydrogen Energy* **2009**, *34*, 929–937. <https://doi.org/10.1016/j.ijhydene.2008.09.105>.
99. Ferreira, M.J.F.; Rangel, C.M.; Pinto, A.M.F.R. Water handling challenge on hydrolysis of sodium borohydride in batch reactors. *Int. J. Hydrogen Energy* **2012**, *37*, 6985–6994. <https://doi.org/10.1016/j.ijhydene.2011.12.028>.
100. Marchionni, A.; Bevilacqua, M.; Filippi, J.; Folliero, M.G.; Innocenti, M.; Lavacchi, A.; Miller, H.A.; Pagliaro, M.V.; Vizza, F. High volume hydrogen production from the hydrolysis of sodium borohydride using a cobalt catalyst supported on a honeycomb matrix. *J. Power Sources* **2015**, *299*, 391–397. <https://doi.org/10.1016/j.jpowsour.2015.09.006>.
101. Lee, C.J.; Kim, T.; Hydrogen supply system employing direct decomposition of solid-state NaBH_4 . *Int. J. Hydrogen Energy* **2015**, *40*, 2274–2282. <https://doi.org/10.1016/j.ijhydene.2014.12.032>.
102. Minkina, V.M.; Shabunya, S.I.; Kalinin, V.I.; Smirnova, A. Hydrogen generation from sodium borohydride solutions for stationary applications. *Int. J. Hydrogen Energy* **2016**, *41*, 9227–9233. <https://doi.org/10.1016/j.ijhydene.2016.03.063>.
103. Cento, C.; Gislou, P.; Prosini, P.P. Hydrogen generation by hydrolysis of NaBH_4 . *Int. J. Hydrogen Energy* **2009**, *34*, 4551–4554. <https://doi.org/10.1016/j.ijhydene.2008.07.088>.
104. Özkan, G.; Akkuş, M.S.; Özkan, G. The effects of operating conditions on hydrogen production from sodium borohydride using Box-Wilson optimization technique. *Int. J. Hydrogen Energy* **2019**, *44*, 9811–9816. <https://doi.org/10.1016/j.ijhydene.2018.12.134>.
105. Zhang, H.; Zhang, L.; Rodríguez-Pérez, I.A.; Miao, W.; Chen, K.; Wang, W.; Li, W.; Han, S. Carbon nanospheres supported bimetallic Pt-Co as an efficient catalyst for NaBH_4 hydrolysis. *Appl. Surf. Sci.* **2021**, *540*, 148296. <https://doi.org/10.1016/j.apsusc.2020.148296>.
106. Ke, D.; Tao, Y.; Li, Y.; Zhao, X.; Zhang, L.; Wang, J.; Han, S. Kinetics study on hydrolytic dehydrogenation of alkaline sodium borohydride catalyzed by Mo-modified Co-B nanoparticles. *Int. J. Hydrogen Energy* **2015**, *40*, 7308–7317. <https://doi.org/10.1016/j.ijhydene.2015.04.041>.
107. Nunes, H.X.; Ferreira, M.J.F.; Rangel, C.M.; Pinto, A.M.F.R. Hydrogen generation and storage by aqueous sodium borohydride (NaBH_4) hydrolysis for small portable fuel cells (H_2 –PEMFC). *Int. J. Hydrogen Energy* **2016**, *41*, 15426–15432. <https://doi.org/10.1016/j.ijhydene.2016.06.173>.

108. Akkuş, M.S.; Murathan, H.B.; Özgür, D.Ö.; Özkan, G.; Göksel Özkan, G. New insights on the mechanism of vapour phase hydrolysis of sodium borohydride in a fed-batch reactor. *Int. J. Hydrogen Energy* **2018**, *43*, 10734–10740. <https://doi.org/10.1016/j.ijhydene.2018.01.177>.
109. Li, F.; Li, J.; Chen, L.; Dong, Y.; Xie, P.; Li, Q. Preparation of CoB nanoparticles decorated PANI nanotubes as catalysts for hydrogen generation from NaBH₄ hydrolysis. *J. Taiwan Inst. Chem. Eng.* **2021**, *122*, 148–156. <https://doi.org/10.1016/j.jtice.2021.04.051>.
110. Chen, Y.-H.; Lin, J.-C. Reactant Feeding Strategy Analysis of Sodium Borohydride Hydrolysis Reaction Systems for Instantaneous Hydrogen Generation. *Energies* **2020**, *13*, 4674. <https://doi.org/10.3390/en13184674>.
111. Li, Q.; Wang, F.; Zhou, X.; Chen, J.; Tang, C.; Zhang, L. Synergistical photo-thermal-catalysis of Zn₂GeO₄:xFe³⁺ for H₂ evolution in NaBH₄ hydrolysis reaction. *Catal. Commun.* **2021**, *156*, 106321. <https://doi.org/10.1016/j.catcom.2021.106321>.
112. Lim, D.; Özkan, G.; Özkan, G. Ni–B and Zr–Ni–B in-situ catalytic performance for hydrogen generation from sodium borohydride, ammonia borane and their mixtures. *Int. J. Hydrogen Energy* **2022**, *47*, 3396–3408. <https://doi.org/10.1016/j.ijhydene.2021.03.039>.
113. Pinto, A.M.F.R.; Ferreira, M.J.F.; Fernandes, V.R.; Rangel, C.M. Durability and reutilization capabilities of a Ni–Ru catalyst for the hydrolysis of sodium borohydride in batch reactors. *Catal. Today* **2011**, *170*, 40–49. <https://doi.org/10.1016/j.cattod.2011.03.051>.
114. Li, R.; Zhang, F.; Zhang, J.; Dong, H. Catalytic hydrolysis of NaBH₄ over titanate nanotube supported Co for hydrogen production. *Int. J. Hydrogen Energy* **2022**, *47*, 5260–5268. <https://doi.org/10.1016/j.ijhydene.2021.11.143>.